DOI: 10.1007/s002670010258

Modeling Urban Growth Effects on Surface Runoff with the Integration of Remote Sensing and GIS

QIHAO WENG*
Department of Geography, Geology, and Anthropology
Indiana State University
Terre Haute, IN 47809, USA

ABSTRACT / A methodology is developed to relate urban growth studies to distributed hydrological modeling using an integrated approach of remote sensing and GIS. This linkage is possible because both studies share land-use and land-cover data. Landsat Thematic Mapper data are utilized to detect urban land-cover changes. GIS analyses are then conducted to examine the changing spatial patterns of urban growth. The integration of remote sensing and GIS is applied to automate the estimation of surface runoff based on the Soil Conservation Service model. Impacts of urban growth on surface runoff and the rainfall–runoff relationship are examined by linking the two modeling results with spatial analysis techniques. This methodology is applied to the Zhujiang Delta of southern China, where dramatic urban growth has occurred over the past two decades, and the rampant urban growth has created severe problems in water resources management. The results revealed a notably uneven spatial pattern of urban growth and an increase of 8.10 mm in annual runoff depth during the 1989–1997 period. An area that experienced more urban growth had a greater potential for increasing annual surface runoff. Highly urbanized areas were more prone to flooding. Urbanization lowered potential maximum storage, and thus increased runoff coefficient values.

Land-use and land-cover changes may have four major direct impacts on the hydrological cycle and water quality: they can cause floods, droughts, and changes in river and groundwater regimes, and they can affect water quality (Rogers 1994). In addition to these direct impacts, there are also indirect impacts on climate and the subsequent impact of the altered climate on the waters. Urbanization, the conversion of other types of land to uses associated with the growth of population and economy, is a significant land-use and land-cover change especially in recent human history. The process of urbanization has a considerable hydrological impact in terms of influencing the nature of runoff and other hydrological characteristics, delivering pollutants to rivers, and controlling rates of erosion (Goudie 1990).

At different stages of urban growth, various impacts can be observed (Kibler 1982). In the early stage of urbanization, removal of trees and vegetation may decrease evapotranspiration and interception and increase stream sedimentation. Later, when construction of houses, streets, and culverts begins, the impacts may include decreased infiltration, lowered groundwater table, increased storm flows, and decreased base flows during dry periods. After the development of residential and commercial buildings has been completed, increased imperviousness will reduce the time of runoff, concentration so that peak discharges are higher and occur sooner after rainfall starts in basins. The volume of runoff and flood damage potential will greatly increase. Moreover, the installation of sewers and storm drains accelerates runoff (Goudie 1990). As a result, the rainfall–runoff process in an urban area tends to be quite different from that in natural conditions depicted in classical hydrological cycles. This effect of urbanization, however, varies according to the size of a flood. As the size of the flood becomes larger and its recurrence interval increases, the effect of urbanization decreases (Hollis 1975).

The integration of remote sensing (RS) and geographic information systems (GIS) has been widely applied and has been recognized as a powerful and effective tool in detecting urban growth (Ehlers and others 1990, Treitz and others 1992, Harris and Ventura 1995, Yeh and Li 1996, 1997). Remote sensing collects multispectral, multiresolution, and multitemporal data, and turns them into information valuable for understanding and monitoring urban land processes and for building urban land-cover data sets. GIS technology provides a flexible environment for entering, analyzing, and displaying digital data from various sources necessary for urban feature identification, change detection, and database development. In hydrological and watershed modeling, remotely sensed data are found to be valuable for providing cost-effective data input and for estimating model parameters (Engman and Gurney 1991, Drayton and others 1992, Mattikalli and others 1996). The introduction of GIS to the field makes it

KEY WORDS: Remote sensing–GIS integration; Urban growth; Surface runoff; Zhujiang Delta; China

*e-mail: geweng@scifac.indstate.edu

possible for computer systems to handle the spatial nature of hydrological parameters. The hydrological community now increasingly adopts GIS-based distributed modeling approaches (Berry and Sailor 1987, Drayton and others 1992, Mattikalli and others 1996). However, no attempt has been made to relate urban growth studies to distributed hydrological modeling, although both studies share land-use and land-cover data. This is especially true in applying an integrated approach of remote sensing and GIS to developing countries such as China.

This paper attempts to develop an integrated approach to remote sensing and GIS to examine the effects of urban growth on surface runoff at the local level. Using the Zhujiang Delta of South China between 1989 and 1997 as a case study, the specific objectives of this paper are: (1) to detect urban land-cover changes using satellite remote sensing and GIS and to study spatial patterns of urban growth; (2) to examine the effect of such urban growth on surface runoff; and (3) to evaluate the impact of urban growth on rainfall–runoff relationship.

Distributed Surface Runoff Model

The model used for estimating surface runoff in this study was developed by the United States Soil Conservation Service (SCS). It has been widely applied to estimate storm runoff depth for every patch within a watershed based on runoff curve numbers (CN) (USDA 1972). The SCS equation for storm runoff depth is mathematically expressed as:

$$Q = \frac{(P - 0.2S)^2}{(P + 0.8S)} \qquad (1)$$

where: Q is storm runoff; P is rainfall; S is potential maximum storage, and $S = (1000/CN) - 10$; CN is runoff curve number of hydrologic soil group–land-cover complex.

To solve this equation, two input values are necessary: P and CN. Precipitation data are often available from meteorological observations. A runoff curve number is a quantitative description of land cover and soil conditions that affect the runoff process. The CN values are normally estimated using field survey data with reference to USDA's SCS tables (Table 1). From Table 1, it is apparent that CN values approaching 100 are associated with high runoff from cultivated agricultural land, whereas low to moderate CN values indicate the reduced runoff from heavily vegetated areas (Slack and Welch 1980). A hydrological soil group code A, B, C, or D was set up by the SCS for over 4000 soils in the United States based on permeability and infiltration characteristics. Group A soils are coarse, sandy, well-drained soils, with the highest rate of infiltration and the lowest potential for runoff. Group D soils, on the other hand, are heavy, clayey, poorly drained soils, with the lowest rate of infiltration and highest potential for runoff. Group B and C soils are intermediate between groups A and D.

Since the availability of Landsat data in the 1970s, several attempts have been made to use these satellite data to determine CNs because of the cost-effective nature of these data. Mintzer and Askari (1980) employed Landsat MSS data, in combination with color infrared photography, to derive the runoff coefficients for the watersheds of Mill Creek in Ohio, USA, by using polynomial regression modeling. Ragan and Jackson (1980) compared the estimation of curve numbers from Landsat MSS with those from field surveys and from high-level aerial photography. It was suggested that there was no significant difference among the three sources, but a modified curve number classification system compatible with Landsat data needs to be established. Slack and Welch (1980) conducted a similar study for the Little River watershed near Tifton, Georgia, USA. They generated four hydrologically important land classes: agricultural vegetation, forest, wetland, and bare ground from Landsat MSS data, and found that curve numbers for six subwatersheds and for the entire watershed were estimated within two curve number units. Rango and others (1983) claimed only a 5% error in land-cover estimation by Landsat data at the basin level, but a much greater error at the cell level.

The development and maturity of GIS technology in the late 1980s have made it possible to combine various data sources for the derivation of model input parameters and have automated the SCS modeling process. Berry and Sailor (1987) used Map Analysis Package (MAP) to automate the procedures for estimating input parameters for Soil Conservation Service method of predicting storm runoff volume and lag to peak timing. Drayton and others (1992) used GIS to develop the runoff model for the Tywi catchment of West Wales, UK, based on a rectangular grid cell network. The incorporation of topographic information allows them to further derive flow routing and to generate a hydrograph. Mattikalli and others (1996) conducted the modeling in a vector GIS environment using Arc/Info, and evaluated the effect of land use change on river discharge by comparing rainfall-runoff curves over time and on water quality as indexed by nitrogen loading.

Table 1. Runoff curve numbers for hydrologic soil-cover complexes (USDA 1972) (antecedent moisture condition II and $I_a = 0.2S$)

Land use	Cover treatment or practice	Hydrologic condition	Runoff curve number for hydrologic soil group			
			A	B	C	D
Fallow	Straight row	—	77	86	91	94
Row crops	Straight row	Poor	72	81	88	91
		Good	67	78	85	89
	Contoured	Poor	70	79	84	88
		Good	65	75	82	86
	Contoured and terraced	Poor	66	74	80	82
		Good	62	71	78	81
Small grain	Straight row	Poor	65	76	84	88
		Good	63	75	83	87
	Contoured	Poor	63	74	82	85
		Good	61	73	81	84
	Contoured and terraced	Poor	61	72	79	82
		Good	59	70	78	81
Close seeded legumes[a] or rotation meadow	Straight row	Poor	66	77	85	89
		Good	58	72	81	85
	Contoured	Poor	64	75	83	85
		Good	55	69	78	83
	Contoured and terraced	Poor	63	73	80	83
		Good	51	67	76	80
Pasture or range		Poor	68	79	86	89
		Fair	49	69	79	84
		Good	39	61	74	80
	Contoured	Poor	47	67	81	88
		Fair	25	59	75	83
		Good	6	35	70	79
Meadow		Good	30	58	71	78
Woods		Poor	45	66	77	83
		Fair	36	60	73	79
		Good	25	55	70	77

[a]Close drilled or broadcast.

Study Area

The study area, the Zhujiang (literally "the Pearl River") Delta, is located between latitudes 21°40′N and 23°N, and longitudes 112°E and 113°20′E (Figure 1). It is the third biggest river delta in China and has an area of 17,200 sq km. Because of the constraints of satellite imagery coverage, this research focuses on the core area of the delta that includes the following 15 cities/counties shown in Figure 1. Geomorphologically, the Zhujiang Delta consists of three subdeltas, the Xijiang (West River), Beijiang (North River), and Dongjiang (East River) Deltas, which originated approximately 40,000 years ago (Department of Geography, Zhongshan University 1988). The process of sedimentation continues today, extending seaward at a rate of 40 m/year (Gong and Chen 1964). The delta has a subtropical climate with an average annual temperature of 21°–23°C, and an average precipitation of 1600–2600 mm. Because of the impact of the East Asian monsoonal circulation, about 80% of the rainfall comes in the period from April to September with a concentration in the months of May, June, and July, when the delta is most prone to flooding (Ditu Chubanshe 1977). Another hazard is typhoons, which occur most frequently from June to October.

The drainage system in the delta is well developed as a result of abundant rainfall. Of the total annual runoff of 341.2 billion m^3, the Xijiang contributes the most (72.10%), followed by the Beijiang (14.13%), and the Dongjiang (9.14%). The annual mean discharge for the Xijiang ranges from 848 to 48,800 m^3/sec; for the Beijiang, it ranges from 139 to 14,900 m^3/sec, and for the Dongjiang, it ranges from 31.4 to 12,800 m^3/sec (Department of Geography, Zhongshan University, 1988). The load discharge of the river system is large, with an annual total silt discharge of 83.36 million tons, of which the Xijiang is the major contributor (87%) (Huang and others 1982). About 20% of the silt dis-

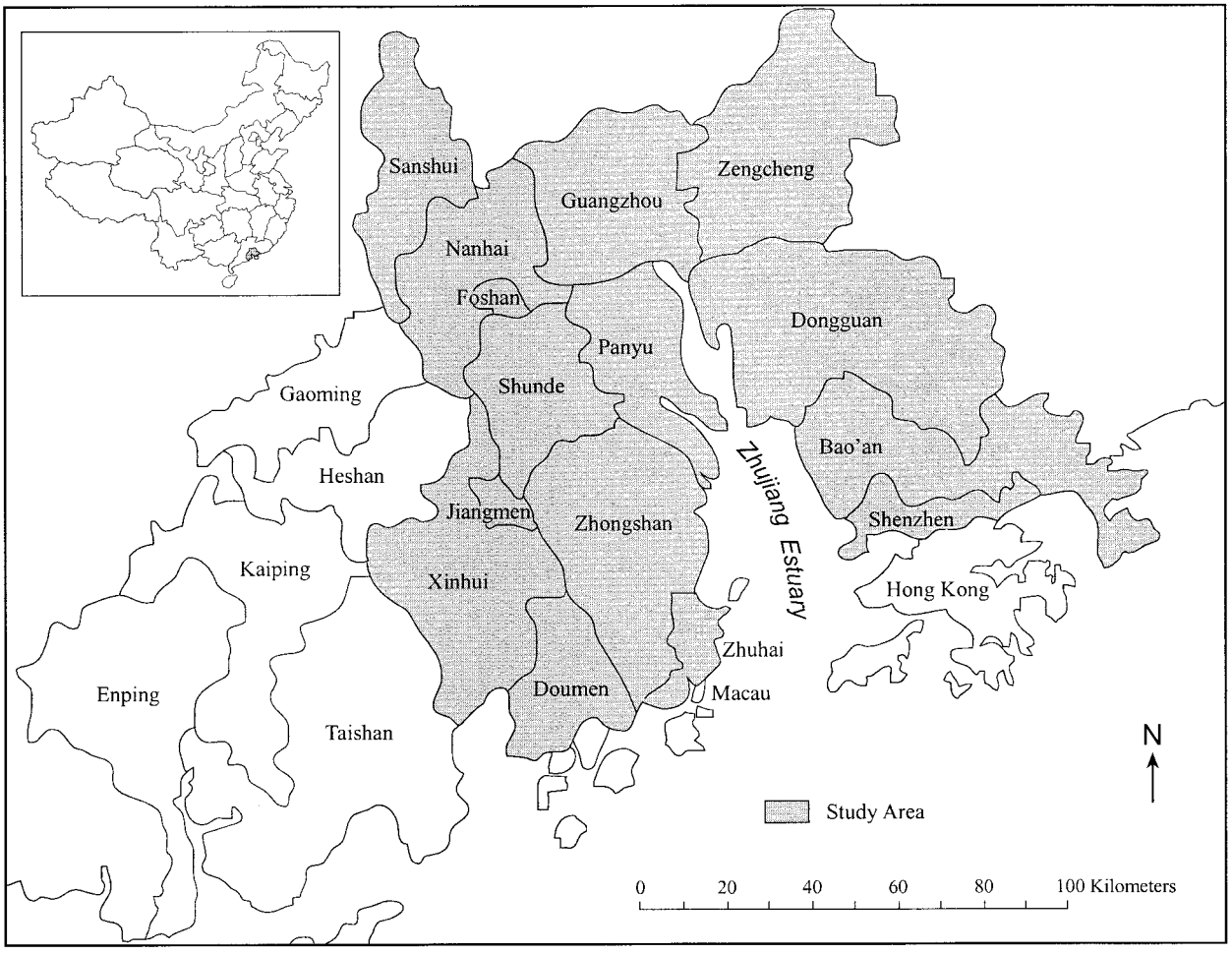

Figure 1. Location of the study area.

charge is deposited in the delta region while 80% enters the sea, thus causing a seaward extension in the mouth region of the Zhujiang. The rivers of the system arrive at the South China Sea through eight estuaries ("gates" in Chinese), namely, Humen, Jiaomen, Hongqili, Hengmen, Modaomen, Jitimen, Hutiaomen, and Yamen from north to south. Perhaps the most distinguishing characteristic of the river system is its numerous tributaries. There are 100 main branches in the system, with a total length of over 1700 km. The drainage density in the Xijiang and the Beijiang deltas is 0.81 km/sq km, and 0.88 km/sq km in the Dongjiang Delta. The average channel width–depth ratio is 1.8 to 11.5. However, 68% of all channels have a ratio of less than 6.0, which indicates that most river channels in the delta are stable. The average channel gradient in all major rivers is low: 0.0023% in the Xijiang, 0.0037% in the Beijiang, and 0.026% in the Dongjiang.

The Delta's fertile alluvial deposits, in combination with the subtropical climate, make it one of the richest agricultural areas in China. A variety of crops, vegetation, cash crops, and fruit trees are the major agricultural products. Agricultural land accounts for almost half of the total area. Known as an ecologically well-integrated agriculture–aquaculture system (Zhong 1980; Ruddle and Zhong 1988), the dike-pond land is a unique landscape feature of the delta, accounting for 4% of the area. Inside the delta, there are over 160 hills and terraces located at heights of 100–300 m above sea level (Huang and others 1982). These hills and terraces are largely occupied by forest (28%) and grassland (15%) (Department of Geography, Zhongshan University 1988). Only a small portion of the land was urban or built-up in 1978. However, urban growth has been speeded up due to accelerated economic development after 1978, when the Chinese government initiated economic reform policies. Massive parcels of agricultural land are disappearing each year for urban or related

uses. Because of the lack of appropriate land-use planning and measures for sustainable development, rampant urban growth has created severe environmental consequences.

Economically, the Zhujiang Delta is the largest area of economic activity in South China. Hong Kong and Macau are located here. Since 1978, the delta has become very important due to its dramatic economic expansion, and therefore has been regarded as a model for Chinese regional development. The establishment of the Shenzhen and Zhuhai Special Economic Zones in 1979 and the Zhujiang Delta Economic Open Zone in 1985 has stimulated Hong Kong and foreign firms to locate their factories there as village-township enterprises. The labor-intensive industries, in association with the cash crop production have transformed the spatial economy of the delta (Lo 1989, Lin 1997, Weng 1998).

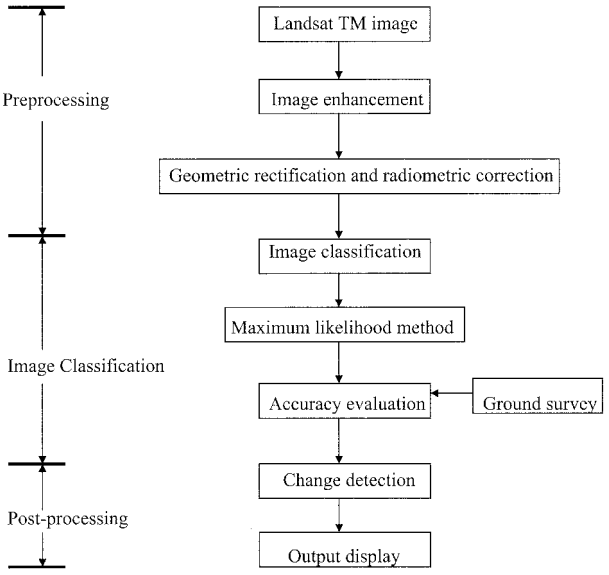

Figure 2. The procedure for deriving land use/cover data and change detection from satellite imagery.

Integrated RS–GIS Approach to Runoff Modeling

Integration of GIS and remote sensing (RS) in runoff modeling involves two processes: (1) hydrological parameter determination using GIS, and (2) hydrological modeling within GIS. Hydrological parameter determination using GIS entails preparing land-cover, soil, and precipitation data that go into the SCS model, while hydrological modeling within GIS automates the SCS modeling process using generic GIS functions. Remote sensing is used for obtaining land-cover data each year and for obtaining information about the nature, rate, and location of land-use and land-cover changes. Urban growth analysis is then carried out by superimposing administrative boundaries on the land-use and land-cover change map. After a surface runoff image is obtained from the hydrological modeling, the technique of image differencing is applied to evaluate the changes in surface runoff over the time. The urban expansion map is overlaid with the runoff change map to analyze the impact of land-use and land-cover change on the environment. These methods and implementation procedures are elaborated below

Hydrological Parameter Determination Using GIS

Derivation of land-cover data and change detection. Land-use and land-cover patterns for 1989 and 1997 were mapped by the use of Landsat Thematic Mapper data (dates: 13 December 1989 and 29 August 1997). A modified version of the Anderson scheme of land use/cover classification that takes into account local conditions (Anderson and others 1976) has been adopted. The categories include: (1) urban or built-up land, (2) barren land, (3) cropland, (4) horticulture farms, (5) dike-pond land, (6) forest, and (7) water. With the aid of Erdas Imagine computer software, each Landsat image was enhanced using linear contrast stretching and histogram equalization to increase the volume of visible information. All images are rectified to a common Universal Transverse Mercator (UTM) coordinate system based on the 1:50,000 scale topographic maps of Guangdong Province produced by the Chinese government. Each image was then radiometrically corrected using a relative radiometric correction method (Jensen 1996). A supervised classification with the maximum likelihood algorithm was conducted to classify the Landsat images using bands 2 (green), 3 (red), and 4 (near infrared). The accuracy of the classification was verified by field checking or comparing with existing land-use and land-cover maps that had been field-checked. A typical implementation procedure for satellite image classification is shown in Figure 2.

In performing land-use and land-cover change detection, a cross-tabulation detection method was employed. A change matrix was produced with the help of Erdas Imagine software. Quantitative areal data of the overall land use/cover changes as well as gains and losses in each category can be compiled. In order to analyze the nature, rate, and location of urban land change, an image of urban and built-up land was extracted from each original land cover image. The two

extracted images were then overlaid and recoded to obtain an urban land cover change (growth) image.

This urban growth image was further overlaid with several geographic reference images to help analyze the patterns and processes of urban expansion, including an image of the county/city boundary, major roads, and major urban centers. These layers were constructed in a vector GIS environment and converted into a raster format (grid size = 30 m). The county/city boundary image was utilized to find urban land change information within each county/city.

Derivation of soil data. The soil data are available in a book entitled "Soils of Guangdong" (Liu 1993), based on results from the second national soils survey done between 1979 and 1990. The soil types were extracted from the 1:2,800,000 provincial soil map and digitized into a polygon coverage and registered to the UTM coordinate system. Ten types of soils are found in the study area, which can be grouped into two major categories: (1) podzolized old and young red earths (39.17%), and (2) noncalcarcous alluvium and paddy soils (60.83%). The former is seen in the uplands with clay accumulation and low base supply known as Udults in soil taxonomy (Soil Conservation Service 1975), and the latter in the floodplains and deltas. Red earths are normally permeable and well drained and can be related to class A or B in the hydrological soil group codes of the SCS classification. Paddy soils have been modified by intensive agricultural activities, and their hydrological properties are subject to human influences. As the fields were reclaimed from the sea at various periods of time, a distinction can be made according to their distances from the sea (Lo and Pannell 1985). Inland fields, enclosed with irrigation dikes, were usually developed earlier than those found along the coast and are more fertile and higher yielding. The fields found near the coast are susceptible to flooding, and their soils tend to be more saline and less suitable for agricultural purposes. The majority of the paddy soils consists of loam or silt loam and can be classified into hydrosoil group C. In most of Shunde County in the central delta, however, a much larger proportion of clay may be found in the soils. These soils are grouped in the class D given their relative weak permeability and infiltration. The hydrological soil group codes (A, B–C, and D) were associated with each polygon in the soil coverage. This coverage was converted into a raster layer with a resolution of 30 m. After the vector-to-raster conversion, a 3 × 3 mode filter was passed over the data layer to eliminate any "slivers" (Lo and Shipman 1990).

Derivation of precipitation data. Rainfall data are available for all cities and counties of the delta in Guangdong Statistical Yearbooks (Guangdong Statistical Bureau 1990, 1998) and Guangdong Province Gazetteer of Geography (Liu 1998). These rain gauges were usually located in the urban center of a county seat or a city proper, and recorded continuous data from the early 1950s. Daily, monthly, and yearly rainfall totals are available for every year. The gauge stations were digitized and registered to the UTM coordinate system. A Theissen polygon coverage (in which two neighboring stations have an equal distance to the boundary) was built using Arc/Info (a vector GIS program) commands. By assigning average yearly rainfall totals to each polygon in the coverage, a rainfall data layer was generated. The data layer was then converted into raster format with a resolution of 30 m.

Hydrological Modeling within GIS

To start modeling, a land cover image and the soil layer were combined and recoded to calibrate CN values with the aid of the standard SCS table (USDA 1972); and a CN image was thus created. By using the map algebra function of the GIS, a potential maximum storage (S) can be computed for each pixel. A layer of potential maximum storage was then created for each year. This layer was further overlaid with the rainfall layer to create a runoff image (Figure 3).

Image differencing was performed between the 1989 and the 1997 runoff layers. The resulting differencing image was reclassified into runoff change zones. The areal extent and spatial occurrence of these zones were studied in reference to the spatial patterns of urban growth in order to understand the effects of land-use and land-cover changes.

Urban growth alters the relationship between rainfall and runoff through potential maximum storage. An average value of potential maximum storage for each city/county was computed by superimposing city/county boundaries on a potential maximum storage layer. Assuming uniform rainfall events from 10 to 100 mm with an increment of 10 mm occurred in each city/county, runoff depths for these events can be calculated based on the SCS model: $Q = (P - 0.2S)^2/(P + 0.8S)$. Runoff coefficients, defined as the ratio of runoff to rainfall, can also be computed for each event. A runoff coefficient curve was constructed as a function of the size of the flood. By comparing the curve in 1989 and in 1997, the effect of urbanization can be examined, showing how it varies according to the size of the flood. By relating runoff coefficient curve patterns and changes with urban growth patterns in each city/county, the effect of urbanization was further studied.

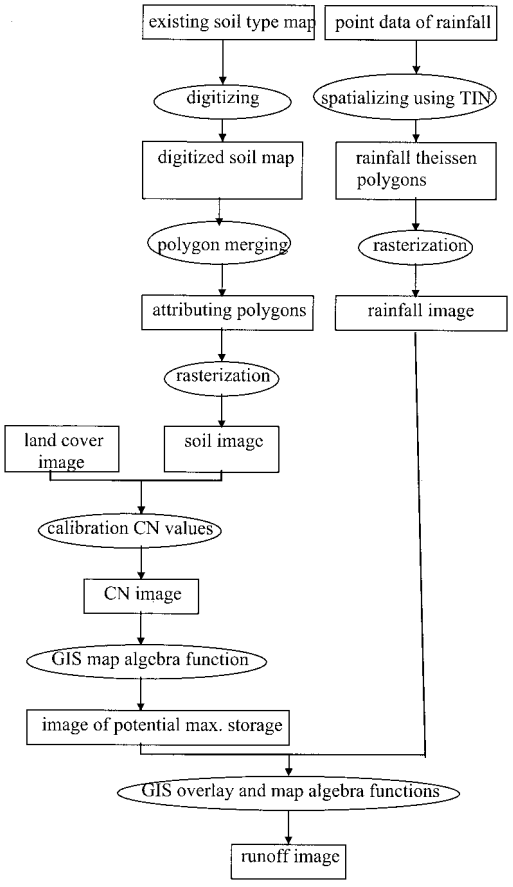

Figure 3. The implementation procedure of GIS-based surface runoff modeling.

Results and Analyses

Urban Growth in the Zhujiang Delta

The RS-GIS analysis indicates that urban or built-up land has expanded by 47.68% percent (65,690 ha) in the delta during 1989–1997. Overlaying the 1989 and 1997 land use/cover maps reveals that most urban or built-up land increases were at the expense of cropland (37.92%) and horticulture farms (16.05%). The overlay of this map with a city/county map reveals the areal extent and spatial occurrence of urban expansion within administrative regions. Table 2 and Figure 4 illustrate the result of this GIS overlay. It is shown that in absolute terms the greatest urban expansion occurred in Dongguan (+23478.90 ha), Bao'an (+14941.08 ha), Nanhai (8004.1 ha), and Zhuhai (+5869.71 ha). However, in percentage terms, the largest increase in urban or built-up land occurred in Zhuhai (1100.00%), followed by Shenzhen (306.65%), Bao'an (233.33%), and Dongguan (125.71%). Massive urban sprawl in these areas can be ascribed to rural areas urbanization of rural areas, a common phenomenon in postreform China. Rapid urban development in the form of small towns on the east side of the delta is highly influenced by investment from Hong Kong. In contrast, the old cities, such as Guangzhou and Foshan, do not show a rapid increase in urban or built-up land because they have no land on which to expand further (as they have already expanded fully in the past) and because of the concentration of urban enterprises in the city proper. Shenzhen and Zhuhai were designated as Special Economic Zones at the same time, but the pace of urbanization in the two cities is quite different. Urban development in Shenzhen was mostly completed in the 1980s, while Zhuhai's urban expansion appeared primarily during the period of 1989–1997 (+5869.71 ha).

Table 2. Satellite-detected urban expansion in the Zhujiang Delta, 1989–1997

City/county	Total area (ha)	Urban area (ha) 1989	Urban area (ha) 1997	Change ha	Change %
Bao'an	159,752	6,403	21,344	14,941	233.33
Dongguan	230,202	18,676	42,155	23,479	125.71
Doumen	55,566	2,134	3,735	1,601	75.00
Foshan	9,922.5	6,403	6,937	534	8.33
Guangzhou	140,900	23,479	28,281	4,802	20.45
Jiangmen	9,923	1,601	3,735	2,134	133.33
Nanhai	106,171	13,340	21,344	8,004	60.00
Panyu	79,380	7,471	8,538	1,067	14.29
Sanshui	91,287	2,134	2,134	0	0.00
Shenzhen	27,783	1,050	4,269	3,219	306.65
Shunde	78,388	6,403	10,139	3,736	58.33
Xinhui	151,814	5,870	7,471	1,601	27.27
Zengcheng	176,621	5,870	5,870	0	0.00
Zhongshan	169,675	13,340	16,542	3,202	24.00
Zhuhai	23,814	534	6,403	5,869	1100.00

Impact of Urban Growth on Surface Runoff

The impacts of land-use and land-cover change on surface runoff were examined by comparing predicted runoff volumes in 1989 with those in 1997. The runoff image of 1997 was subtracted from that of 1989. The resulting image of change indicated that the annual runoff volume had increased by 8.10 mm during the 8-year period due to land-use and land-cover changes. This number refers to a uniform runoff depth for the whole delta, and it has a standard deviation of 9.57 mm.

To understand the spatial pattern of the surface runoff changes, the change image was reclassified into ten categories (Table 3). Each of these categories is a set of contiguous or discontinuous locations that exhibit the same value, and each is conventionally called

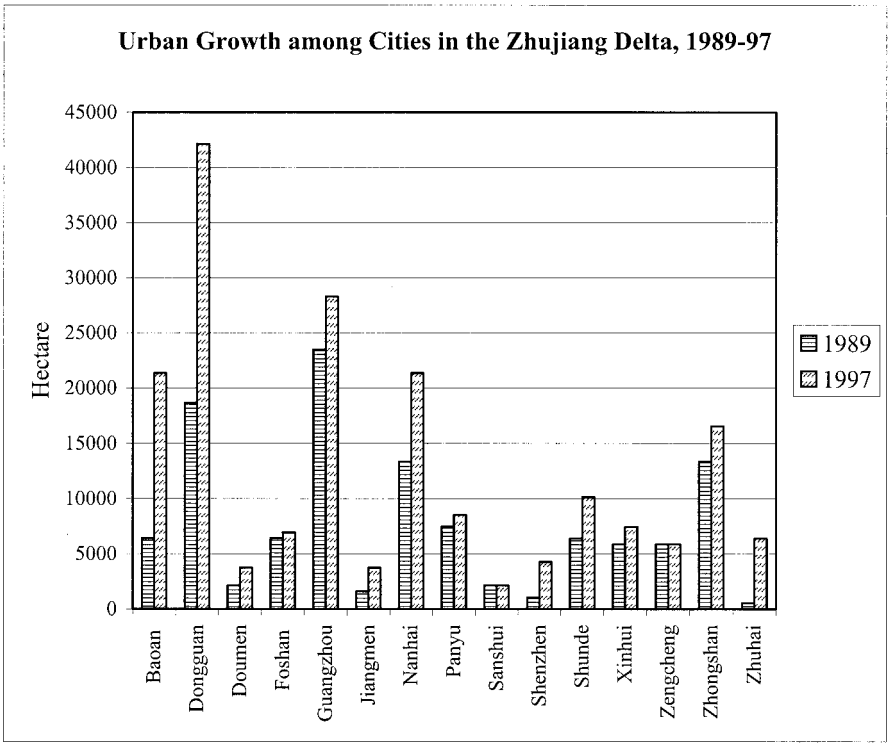

Figure 4. Urban growth among cities in the Zhujiang Delta, 1989–1997.

Table 3. Class assignments of the runoff change image

Runoff change value	Runoff zone
< -3.9	1
-3.9 to -2.9	2
-2.9 to -1.9	3
-1.9 to -0.9	4
-0.9 to 0.1	5
0.1 to 1.1	6
1.1 to 2.1	7
2.1 to 3.1	8
3.1 to 4.1	9
4.1	10

a zone in raster GIS. Zone 1 has the largest negative value (<-3.9 mm), indicating a decrease in runoff change, while zone 10 has the largest positive value (4.1 mm), indicating an increase in surface runoff. A visual interpretation of the areal extent and spatial occurrence of these zones (Figure 5) implies a similarity between the urban expansion pattern and the spatial pattern created by aggregating zones 8–10. These three zones have an increase in the value of surface runoff volume ranging from 2.10 to 24.59 mm, occupying 3.33% of the total area of the delta. By superimposing a city/county map onto these changed runoff zones, the percentages of the aggregated runoff zone in total city/county area were computed. A correlation analysis was then carried out to examine the relationship between the distribution of the aggregated runoff zone and that of urban expansion within each city and county. The result showed a relatively strong positive correlation between the two mapped patterns with a multiple r value of 0.67 (significant at the 0.05 level). This correlation suggests that the more urban growth a city or county experienced, the greater potential it had to increase surface runoff.

Impact of Urban Growth on Rainfall–Runoff Relationship

Figure 6 shows the runoff coefficient as a function of rainfall from 10 to 100 mm in each city/county in 1989–1997. The cities/counties with greater urban growth, such as Shenzhen, Zhuhai, and Bao'an, have a distinctive curve for 1989 from that for 1997. In contrast, those cities/counties with less urban growth have two similar curves. This is particularly true in Zengeheng, Sanshui, Panyu, and Xinhui, where the two curves are so similar that visual differentiation is nearly impossible. According to the SCS model, the rainfall–runoff relationship is controlled by potential maximum storage. Therefore, the effect of urban growth on the relationship can be studied by relating the following

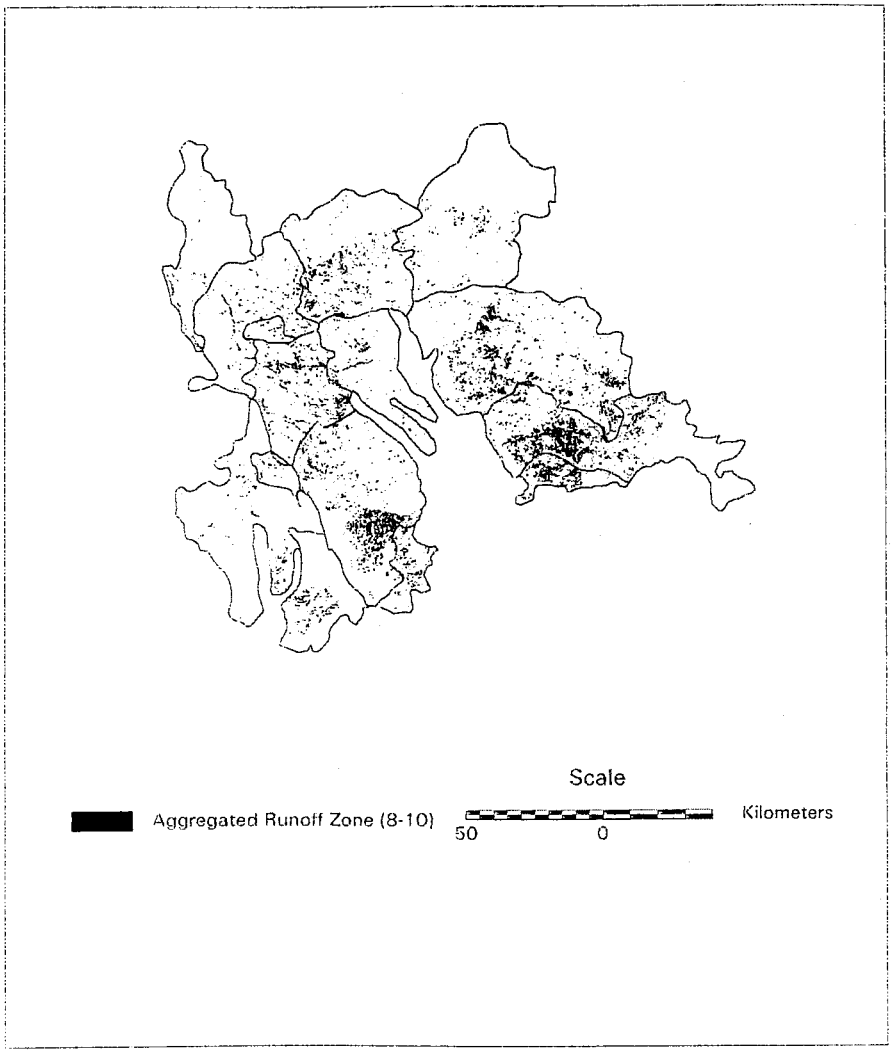

Figure 5. Surface runoff changes in the Zhujiang Delta, 1989–1997.

two variables: changes in potential maximum storage value and urban growth rates (percentage of urban growth). A correlation analysis between them gives a multiple r value of 0.6 (significant at the 0.05 level). This result suggests that urban growth was a major contributor to the changes in potential maximum storage and thus in the relationship between rainfall and runoff.

A city or county with a higher degree of urbanization (ratio of urbanized area to total area) has generally a lower average value of potential maximum storage, and vice versa. A correlation between the two sets of variables gives $r = 0.56$ in 1989, and the coefficient increases to -0.68 by 1997. This increase is a good indication that urbanization has played an increasingly important role in shaping the relationship of rainfall to runoff. Furthermore, highly urbanized areas (such as Foshan, Jiangmen, and Zhuhai) are more prone to flooding than less urbanized ones (such as Sanshui, Zengcheng, Xinhui, and Doumen). This is because lower values in potential maximum storage often imply that the same amount of rainfall will generate more runoff. Foshan City in the central delta, for example, had an urbanization degree of 65% in 1989 and 70% in 1997. Its average runoff coefficient reached 0.46 (SD = 0.034) in 1989, and 0.47 (SD = 0.028) in 1997. The impact of urbanization on runoff can be further examined by comparing runoff coefficient curves (Figure 6). Foshan and Jiangmen have found two highly similar curves, indicating that the degree of urbanization was alike in both 1989 and 1997. Indeed, these cities have long been designed to function as pure urban centers, supported by secondary and tertiary production. The majority of the land near the urban centers was filled before 1978. Recent urban development in these cities

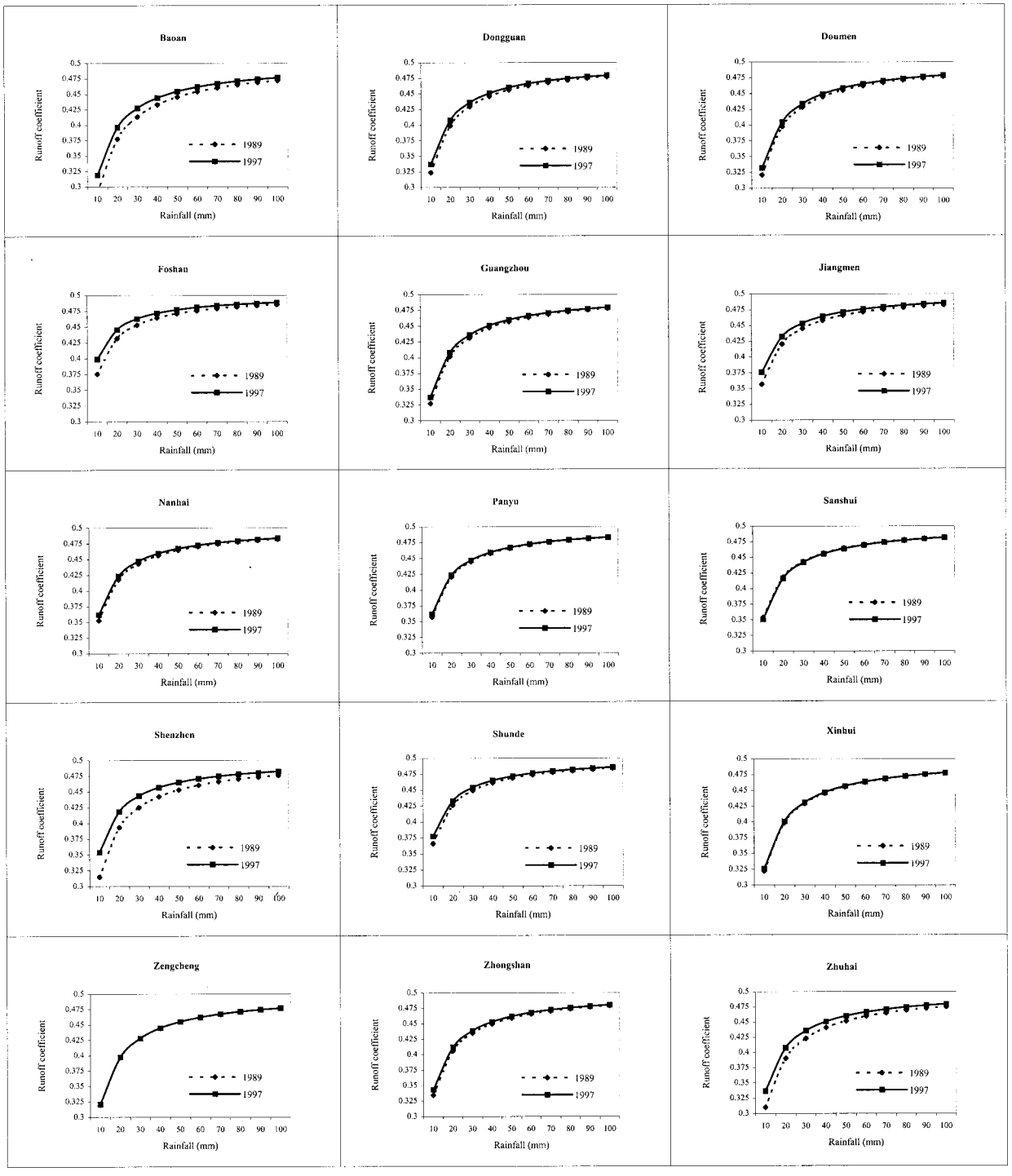

Figure 6. Runoff coefficient as a function of rainfall from 10 to 100 mm.

has had to seek spare land in the suburban areas and is limited to a small scale. Similar runoff coefficient curves can also be identified between Shenzhen and Zhuhai. Both cities were small towns before 1978. Urban development in these cities therefore has had much more freedom and is subject to the influence of the economic reform policies. From satellite imagery, a scattered pattern can be detected in these cities, in which urban development has spread to the suburban and surrounding rural areas.

Conclusions

This paper has focused on the development of an integrated approach of remote sensing and GIS for urban growth study and for distributed hydrological modeling. It has also established the linkage between the two through spatial analysis. By applying this methodology to the Zhujiang Delta of China, urban growth, which resulted from a rapid industrialization, and its relationship to surface runoff have been examined.

The combined use of remote sensing and GIS proves to be an effective tool for urban growth analysis. The technique of detecting land-use and land-cover change can be refined to determine the nature, rate, and location of urban growth. GIS allows for determining the magnitude of satellite-derived urban growth rates within administrative units. Results show that there was a remarkable expansion in urban land cover in the delta between 1989 and 1997, and urban land development was extremely uneven among administrative units.

The integration of GIS and remote sensing has successfully been applied to surface runoff modeling. This study uses GIS to derive two key parameters: rainfall and hydrosoil groups. Based on these data and land-cover digital data, the surface runoff images may be obtained through the map algebra and overlay functions of GIS. Thus, the integration has automated the SCS modeling. Results indicate that annual runoff depth had increased by 8.10 mm between 1989 and 1997. The more urban growth a city or county experienced, the greater potential it had to increase surface runoff. Urban growth has played a critical role in the changing relationships between rainfall and surface runoff.

The missing linkage between urban growth analysis and surface runoff modeling has hindered modeling and assessing the dynamics of land-use and land-cover change and significantly impeded progress towards understanding of earth–atmosphere interactions and global environmental change. This paper demonstrates that the effects of urban growth on surface runoff can be modeled at local levels using the integrated approach of remote sensing and GIS. This linkage is based on the fact that land-use and land-cover data are the main input parameters for both urban growth analysis and surface runoff modeling and that remote sensing and GIS are appropriate techniques for spatial data acquisition and handling. The methodology developed in this paper provides an alternative to traditional empirical observations and analysis using *in situ* (field) data for environmental studies. Future research efforts should validate these spatial modeling results, and investigate the possibility and feasibility that the integration of remote sensing and GIS can be applied in a regional and global context.

Acknowledgments

The funding support provided by the National Geographic Society for the fieldwork of this study through Dr. C. P. Lo is greatly appreciated. The author would also like to acknowledge the financial support of the Research Advisory Committee at the University of Alabama. Last but not least, the author wishes to express his gratitude to Drs. Nina Burkardt, Vaclav Smil, and an anonymous reviewer for their constructive comments and suggestions, which have helped to improve the paper.

Literature Cited

Anderson, J. R., E. E., Hardy, J. T., Roach, and R. E. Witmer. 1976. A land use and land cover classification systems for use with remote sensing data. USGS Professional Paper 964.

Berry, J. K., and J. K. Sailor. 1987. Use of a Geographic Information System for storm runoff prediction from small urban watersheds. *Environmental Management* 11:21–27.

Department of Geography, Zhongshan University. 1988. The Land and Water Resources in the Zhujiang Delta. Zhongshan University Press, Guangzhou.

Ditu Chubanshe (The Map Production Society). 1977. Provincial Atlas of the People's Republic of China. People's Printer, Beijing.

Drayton, R. S., B. M. Wilde, and J. H. K. Harris. 1992. Geographic information system approach to distributed modeling. *Hydrological Processes* 6:36–368.

Ehlers, M., M. A., Jadkowski, R. R., Howard, and D. E. Brostuen. 1990. Application of SPOT data for regional growth analysis and local planning. *Photogrammetric Engineering and Remote Sensing* 56(2):175–180.

Engmen, E. T., and R. J. Gurney. 1991. Remote sensing in hydrology. Chapman & Hall, London.

Gong, Z., and Z. Chen. 1964. The soils of the Zhujiang Delta. *Journal of Soils* 36:69–124 (in Chinese).

Goudie, A. 1990. The human impact on the natural environment, 3rd ed. The MIT Press, Cambridge, Massachusetts.

Guangdong Statistical Bureau. 1990. Statistical yearbook of Guangdong 1989. China Statistics Press, Beijing.

Guangdong Statistical Bureau. 1998. Statistical yearbook of Guangdong 1997. China Statistics Press, Beijing.

Harris, P. M., and S. J. Ventura. 1995. The integration of geographic data with remotely sensed imagery to improve classification in an urban area. *Photogrammetric Engineering and Remote Sensing* 61(8):993–998.

Hollis, G. E. 1975. The effects of urbanization on floods of different recurrence interval. *Water Resources Research* 11: 431–435.

Huang, Z., Li, P., Z., Zhang, K. Li, and P. Qiao. 1982. The formation, development, and evolution of Zhujiang Delta. Kexue Puji Press Guangzhou Branch, Guangzhou (in Chinese).

Jensen, J. R. 1996. Introductory digital image processing: A remote sensing perspective, (2 ed.). Prentice Hall, Upper Saddle River, New Jersey.

Kibler, D. F. (ed.) 1982. Urban stormwater hydrology. American Geophysical Union, Washington, DC.

Lin, G. C. S. 1997. Red capitalism in South China: Growth and development of the Pearl River Delta. UBC Press, Vancouver, Canada.

Liu, A. 1993. The soils of Guangdong. Science Press, Beijing (in Chinese).

Liu, N. 1998. Guangdong Province gazetteer of geography (draft). Department of Geography, South China Normal University, Guangzhou (in Chinese).

Lo, C. P. 1989. Recent spatial restructuring in Zhujiang Delta, South China: A study of socialist regional development strategy. *Annals of the Association of the American Geographers* 79(2):293–308.

Lo, C. P., and C. W. Pannell. 1985. Seasonal agricultural land use patterns in China's Pearl River Delta from multi-date Landsat images. *GeoJournal* 10(2):183–195.

Lo, C. P. and R. L. Shipman. 1990. A GIS approach to land-use change dynamics detection. *Photogrammetric Engineering and Remote Sensing* 56(11):1483–1491.

Mattikalli, N. M., B. J. Devereux, and K. S. Richards. 1996. Prediction of river discharge and surface water quality using an integrated geographic information system approach. *International Journal of Remote Sensing* 17(4):683–701.

Mintzer, O., and F. Askari. 1980. A remote sensing technique for estimating watershed runoff. US Department of Commerce, Washington, DC.

Ragan, R. M., and T. J. Jackson. 1980. Runoff synthesis using Landsat and SCS model. *Journal of Hydraulic Division of the American Society of Civil Engineers* 106:667–678.

Rango, A., A., Feldman, T. S. George, and R. M. Ragan. 1983. Effective use of Landsat data in hydrological models. *Water Resources Bulletin* 19:165–174.

Rogers, P. 1994. Hydrology and water quality. Pages 231–258 *in W. B. Meyer and B. L. Turner II (eds.)*, changes in land use and land cover: A global perspective. Cambridge University Press, Cambridge.

Ruddle, K., and G. Zhong. 1988. Integrated agriculture–aquaculture in South China: The dike-pond system of the Zhujiang Delta. Cambridge University Press, Cambridge.

Slack, R. B., and R. Welch. 1980. Soil conservation service runoff curve number estimates from LANDSAT data. *Water Resources Bulletin* 16(5):887–893.

Soil Conservation Service. 1975. Soil taxonomy. US Department of Agriculture, Washington, DC.

Treitz, P. M., P. J. Howard, and P. Gong. 1992. Application of satellite and GIS technologies for land-cover and land-use mapping at the rural-urban fringe: A case study. *Photogrammetric Engineering and Remote Sensing* 58(4):439–448.

USDA. 1972. National engineering handbook, section 4, hydrology. USDA, Soil Conservation Service. US Government Printing Office, Washington, DC.

Weng, Q. 1998. Local impacts of the post-Mao development strategy; The case of the Zhujiang Delta, southern China. *International Journal of Urban and Regional Studies* 22(3):425–442.

Yeh, A. G. O., and X. Li. 1996. Urban growth management in the Pear River delta—an integrated remote sensing and GIS approach. *The ITC Journal* 1:77–85.

Yeh, A. G. O., and X. Li. 1997. An integrated remote sensing-GIS approach in the monitoring and evaluation of rapid urban growth for sustainable development in the Pearl River Delta, China. *International Planning Studies* 2(2):193–210.

Zhong, G. 1980. The mulberry dike-fish pond system in the Zhujiang Delta: A man-made ecosystem of land-water interaction. *Acta Geographica Sinica* 35(3):200–212.